Noise in integrate-and-fire neurons: from stochastic input to escape rates

Hans E. Plesser*
MPI für Strömungsforschung
Bunsenstrasse 10, D-37073 Göttingen, Germany

Wulfram Gerstner†
MANTRA Center for Neuromimetic Systems
Swiss Federal Institute of Technology, EPFL/DI
CH-1015 Lausanne, Switzerland

March 30, 1999

Abstract

We analyze the effect of noise in integrate-and-fire neurons driven by time-dependent input, and compare the diffusion approximation for the membrane potential to escape noise. It is shown that for time-dependent sub-threshold input, diffusive noise can be replaced by escape noise with a hazard function that has a Gaussian dependence upon the distance between the (noise-free) membrane voltage and threshold. The approximation is improved if we add to the hazard function a probability current proportional to the derivative of the voltage. Stochastic resonance in response to periodic input occurs in both noise models and exhibits similar characteristics.

`Almost accepted for publication in Neural Computation.`

*Corresponding author, plesser@chaos.gwdg.de
†Wulfram.Gerstner@epfl.ch

1 Introduction

Given the enormous number of degrees of freedom in single neurons due to millions of ion channels, and thousands of presynaptic signals impinging on the neuron, it seems natural to describe neuronal activity as a stochastic process (Tuckwell 1989). Since in most neurons the output signal consists of stereotypical electrical pulses (spikes), the theory of point processes has long been employed to analyze neuronal activity (Perkel et al. 1967; Johnson 1996).

The simplest point process model of neural responses to stimuli is that of an inhomogeneous Poisson process with an instantaneous firing rate which depends on the stimulus, and thus on time. Models of this type have successfully been employed to characterize neural activity in the auditory system (Siebert 1970; Johnson 1980; Gummer 1991), and to investigate the facilitation of signal transduction by noise, a phenomenon known as stochastic resonance (Collins et al. 1996). Stevens and Zador (1996) have recently suggested that in the limit of very low firing rates Poisson models of neuronal activity indeed capture most of the dynamics of more complex models.

On the other hand, much recent research indicates that the precise timing of neuronal spikes plays a prominent role in information processing (Rieke et al. 1997). Thus, spiking neuron models are required which provide more insight into the relation between the input current a neuron receives and the spike train it generates as output. In short, these model neurons generate an output spike whenever the membrane potential v, driven by an input current I, reaches a threshold Θ; afterwards the potential v is reset to some value v_{res}. For a recent review, see Gerstner (1998b).

The archetypical spiking neuron model is the integrate-and-fire neuron introduced by Lapicque, see Tuckwell (1988). Stein (1965) first replaced a continuous input current with more realistic random sequences of excitatory and inhibitory input pulses. If each pulse is small and a large number of pulses impinges on the neuron per membrane time constant, the effective input to the neuron can be described by a time-dependent deterministic current $I(t)$ and additive noise $\xi(t)$, which is taken to be Gaussian. In this limit, the evolution of the membrane potential from reset to threshold is a time-dependent Ornstein-Uhlenbeck process with the threshold as an absorbing boundary (Johannesma 1968; Lánský 1997). We will refer to this as the diffusion approximation of neuronal activity.

The separation of the total input current into a deterministic part $I(t)$ and noise is much less clear-cut in neuronal modeling than in physical processes such as Brownian motion. Recent research suggests that the variability of input spike arrival times plays a much greater role than intrinsic noise (Mainen and Sejnowski 1995; Bryant and Segundo 1976). Stochastic spike arrival may arise in noise-free networks with heterogeneous connections as shown in recent theoretical studies (van Vreeswijk and Sompolinski 1996; Brunel and Hakim 1998). In these studies balanced excitation and inhibition prepared the neuron in a state which is just subthreshold. Spikes are then triggered by the fluctuations in the input. Neurons in this regime have a large coefficient of variation just as cortical neurons; for a recent review see König et al. (1996).

The subthreshold regime is also particularly interesting from the point of view of information transmission. Neurons optimally detect temporal information if the mean membrane potential is roughly one standard deviation of the noise below threshold (Kempter et al. 1998). The improvement of signal transduction by noise, known as stochastic resonance, also appears to be limited to this regime (Bulsara and Zador 1996). In the following we will therefore focus on neurons driven by weakly sub-threshold input, i.e. neurons that would be silent in the absence of noise.

In this work, we take the diffusion approximation sketched above as the reference model for neuronal noise. A disadvantage of this model is that it is difficult to solve analytically, particularly for time-dependent input $I(t)$. The interval distribution for a given input $I(t)$ is mathematically equivalent to a first-passage-time problem which is known to be hard. Our aim in this study is to replace the stochasticity introduced by the diffusion term by a mathematically more tractable inhomogeneous point process. To this end, we investigate various escape processes across the firing threshold. An escape process is completely described by a hazard function $h(t)$ which depends only on the momentary values of the membrane potential $v(t)$ and and the input current $I(t)$. We want to identify that function h which reproduces as closely as possible the behavior of the diffusion model, for both periodic and aperiodic inputs. We demonstrate that the optimal hazard function not only reproduces the generation of individual spikes well, but that complex response properties such as stochastic resonance are preserved.

2 Integrate-and-fire neuron models

2.1 Diffusion model

Between two output spikes, the membrane potential of an integrate-and-fire neuron receiving input $I(t)$ evolves according to the following Langevin equation (Tuckwell 1989)

$$\dot{v}(t) = -v(t) + I(t) + \sigma\xi(t)\ . \tag{1}$$

Upon crossing the threshold, $v(t) = 1$, a spike is recorded and the potential reset to $v = 0$. $\xi(t)$ is Gaussian white noise with autocorrelation $\langle \xi(t)\xi(t')\rangle = \delta(t-t')$. The diffusion constant σ is the root mean square (rms) amplitude of this background noise. Note that we have used dimensionless units above, i.e. time is measured in units of the membrane time constant, while voltage is given in terms of the threshold Θ. As a consequence of the diffusion approximation, the input $I(t)$ will not contain any δ-pulses, and $v(t)$ follows continuous trajectories from reset potential to threshold.

Let us denote the firing time of the last output spike by t^*. In the noise-free case ($\sigma = 0$), the potential $v(t)$ for $t > t^*$ depends on the input $I(t')$ for $t^* < t' < t$ and can be found by integration of (1)

$$v_0(\tau|t^*, I(\cdot)) = \mathrm{e}^{-\tau} \int_0^{\tau} I(t^* + s)\, \mathrm{e}^{s}\, \mathrm{d}s\ . \tag{2}$$

Our notation makes explicit that the noise-free trajectory can be calculated given the last firing time t^* and the input I. The subscript 0 is intended to remind the reader that (2) describes the *noise-free* trajectory. The next output spike of the noiseless model would occur at a time $t^* + \tau$ defined by the first threshold crossing,

$$\tau = \min\{\tau' > 0 \,|\, v_0(\tau'|t^*, I(\cdot)) \geq 1\}\ . \tag{3}$$

In the presence of noise, the actual membrane trajectory will fluctuate around the reference trajectory (2) with a variance of the order of σ. We can no longer predict the exact timing of the next spike, but we may ask for the probability distribution $\rho(\tau|t^*, I(\cdot))$

that a spike occurs at $t^* + \tau$, given that the last spike was at t^* and the current is $I(t')$ for $t^* < t' < t^* + \tau$:

$$\rho(\tau|t^*, I(\cdot))\Delta\tau = \Pr \left\{ \begin{array}{l} \text{Spike in } [t^* + \tau, t^* + \tau + \Delta\tau) \text{ given the last reset at } t^* \\ \text{and input } I(t^* + \tau'),\ \tau' > 0. \end{array} \right\} . \tag{4}$$

Our notation makes explicit that no information about the past of the neuron going farther back than the last firing/reset at t^* is needed. We may think of equation (4) as a conditional inter-spike-interval distribution (ISI). For the diffusion noise model, analytical expressions for the interval distributions are not known, except for some rare special cases (Tuckwell 1989). It is, however, possible to calculate these inter-spike-interval distributions numerically based on Schrödinger's renewal ansatz (Plesser and Tanaka 1997; Linz 1985). Source code is available from the authors upon request. In the following we will use the diffusion model as the reference noise model.

If there were no absorbing threshold, equation (1) would describe free diffusion with drift. Then, the pertaining Fokker-Planck equation

$$\begin{aligned} \frac{\partial}{\partial\tau}\mathcal{P}_f\left(v, t^* + \tau \,|\, t^*\right) = &-\frac{\partial}{\partial v}\left[-v + I(t^* + \tau)\right]\mathcal{P}_f\left(v, t^* + \tau \,|\, t^*\right) \\ &+ \frac{D}{2}\frac{\partial^2}{\partial v^2}\mathcal{P}_f\left(v, t^* + \tau \,|\, t^*\right) \end{aligned} \tag{5}$$

with boundary conditions $\lim_{v\to\pm\infty} \mathcal{P}_f\left(v, t^* + \tau \,|\, t^*\right) = 0$ has the solution

$$\mathcal{P}_f\left(v, t^* + \tau \,|\, t^*\right) = \frac{1}{\sqrt{2\pi\eta^2(\tau)}} \exp\left\{-\frac{[v - v_0(\tau|t^*, I(\cdot))]^2}{2\eta^2(\tau)}\right\} , \tag{6}$$

where $\eta^2(\tau) = \frac{\sigma^2}{2}\left(1 - \mathrm{e}^{-2\tau}\right)$. As the exponential term in $\eta(\tau)$ decays at twice the rate of those in $v_0(\tau|t^*, I(\cdot))$, we may approximate for $\tau \gg 1$

$$\mathcal{P}_f\left(v, t^* + \tau \,|\, t^*\right) \approx \frac{1}{\sqrt{\pi}\sigma} \exp\left\{-\frac{[v - v_0(\tau|t^*, I(\cdot))]^2}{\sigma^2}\right\} . \tag{7}$$

2.2 Escape noise and hazard functions

In a noise-free model, the membrane trajectory $v_0(\tau|t^*, I(\cdot))$ is given by equation (2), and the time of the next spike determined by equation (3). In the presence of noise, firing is no longer precise but may occur even though the noise-free trajectory has not yet reached threshold. A simple intuitive noise model can be based on the idea of an escape probability: At each moment of time, the neuron may fire with an instantaneous rate h which depends on the momentary distance between the noise-free trajectory v_0 and the threshold, and possibly the momentary input current as well. More generally, we may introduce a *hazard function* $h(\tau|t^*, I(\cdot))$ which describes the risk of escape across the threshold and depends on the last firing time t^* and the input $I(t')$ for $t^* < t' < t^* + \tau$. Once we know the hazard function, the ISI distribution is given by (Cox and Lewis 1966)

$$\rho(\tau|t^*, I(\cdot)) = h(\tau|t^*, I(\cdot)) \exp\left[-\int_0^\tau h(s|t^*, I(\cdot))\mathrm{d}s\right] . \tag{8}$$

The exponential term accounts for the probability that a neuron survives from t^* to $t^* + \tau$ without firing; the factor $h(\tau|t^*, I(\cdot))$ gives the rate of firing at $t^* + \tau$, provided that the neuron has survived thus far.

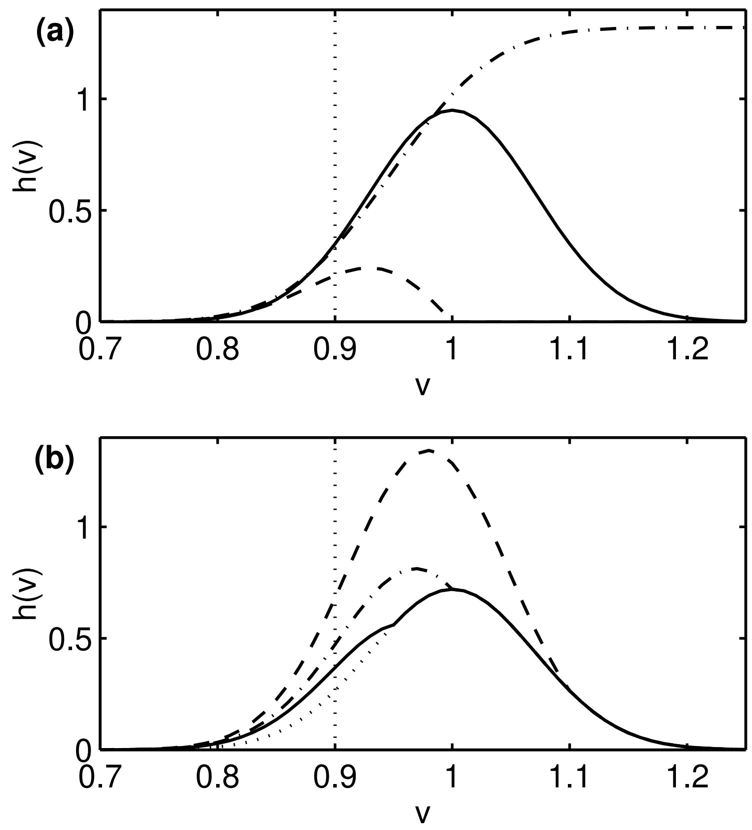

Figure 1: Hazard functions $h(v)$ vs. membrane potential v. (a) Arrhenius model (solid), error function model (dash-dotted) and Tuckwell model (dashed). (b) Arrhenius&Current model for different values of the input current: $I = 0.95$ (solid), 1 (dash-dotted) and 1.1 (dashed); the case $I = 0$ is drawn dotted for comparison. In all cases, the threshold is at $v = 1$ and the noise amplitude is $\sigma = 0.1$. The vertical dotted lines mark one noise amplitude below threshold.

We discuss in this work four models of simplified neuronal dynamics, all of which aim to approximate the diffusion model by an escape noise ansatz. The various models differ in the choice of the function $h(\tau|t^*, I(\cdot))$, see Fig. 1. These hazard functions depend on the noise-free membrane potential v_0 and the input current I only through two scaled quantities. One is the momentary distance x between the membrane potential v_0 and the threshold $\Theta = 1$, scaled by the noise amplitude,

$$x(\tau|t^*) = \frac{1 - v_0(\tau|t^*)}{\sigma} \ . \tag{9}$$

The other is the net current charging the membrane in the noise-free case, also scaled by the noise amplitude,

$$Y(\tau|t^*) = \frac{-v_0(\tau|t^*) + I(t^* + \tau)}{\sigma} = \frac{1}{\sigma}\frac{\mathrm{d}}{\mathrm{d}\tau} v_0(\tau|t^*) \ . \tag{10}$$

The last equality follows immediately from equation (1) with $\sigma = 0$ and indicates that Y can be interpreted as a relative velocity of the noise-free membrane potential v_0.

2.2.1 Arrhenius model

As long as the membrane potential v stays sufficiently far below threshold, we may describe neuronal firing as a noise activated process. The latter is most easily characterized by an Arrhenius ansatz for the hazard function (van Kampen 1992)

$$h_{\mathrm{Arr}}(\tau|t^*) = w \exp\left\{-\frac{(1-v_0(\tau|t^*))^2}{\sigma^2}\right\} = w\,\mathrm{e}^{-x(\tau|t^*)^2}\ ,\ w^{\mathrm{opt}} = 0.95\ . \tag{11}$$

Here, $1 - v_0(\tau|t^*)$ is the voltage gap that needs to be bridged to initiate a spike. Its square may be interpreted as the required activation energy, and σ^2 as the energy supplied by the noise. The free parameter w was determined via an optimization procedure described below. We found $w = w^{\mathrm{opt}} = 0.95$ to be the optimal value. Note that for strongly superthreshold stimuli ($v_0 \gg 1$) the hazard function vanishes exponentially. This might seem paradoxical at first, but is of little concern as long as the input $I(t)$ contains no δ-pulses and v_0 reaches the threshold only along continuous trajectories. Then, superthreshold levels of the potential are accessible only via periods of maximum hazard, so that the neuron will usually have fired before v_0 becomes significantly superthreshold.

2.2.2 Arrhenius&Current model

Strong positive transients in the input current will push the membrane potential towards and across the threshold in a time that is short on the time-scale of diffusion. Figuratively speaking, the membrane potential distribution $\mathcal{P}_f$ is shifted as a whole. The simple Arrhenius ansatz will not be able to reproduce these transients well. We thus consider, in addition to the diffusive current, the probability current induced by shifting the probability density at the threshold, $\mathcal{P}_f\,(\Theta = 1, \tau\,|\,t^*)$, across threshold with the speed of the center of this distribution, $\frac{\mathrm{d}}{\mathrm{d}\tau} v_0(\tau|t^*) = -v_0(\tau|t^*) + I(t^* + \tau)$. Since there can be no drift from above threshold downwards, we set all negative currents to zero and obtain the drift probability current

$$J_{\mathrm{drift}}(\tau|t^*) = [-v_0(\tau|t^*) + I(t^*+\tau)]_+\,\mathcal{P}_f\,(\Theta = 1, \tau\,|\,t^*) = \frac{[Y(\tau|t^*)]_+}{\sqrt{\pi}}\,\mathrm{e}^{-x(\tau|t^*)^2}\ .$$

$\mathcal{P}_f\,(v, \tau\,|\,t^*)$ is again the free Gaussian distribution given by (7) and $[x]_+ \equiv (x + |x|)/2$. Together with the original, diffusive Arrhenius term we obtain the hazard function

$$\begin{aligned} h_{\mathrm{AC}}(\tau|t^*) &= h_{\mathrm{Arr}}(\tau|t^*) + J_{\mathrm{drift}}(v, \tau|t^*) \\ &= \left(w + \frac{[Y(\tau|t^*)]_+}{\sqrt{\pi}}\right)\mathrm{e}^{-x(\tau|t^*)^2}\ , \quad w^{\mathrm{opt}} = 0.72\ . \end{aligned} \tag{12}$$

As before w is a free parameter with optimal value w^{opt}. Below we will refer to the first term of (12) as the diffusion term and to the second one as the drift term.

2.2.3 Sigmoidal model

Abeles (1982) has suggested that the hazard should be related to the proportion of the free membrane potential distribution $\mathcal{P}_f$ that is beyond the threshold, i.e. $h(\tau|t^*) \sim \int_\Theta^\infty \mathcal{P}_f\,(v, \tau\,|\,t^*)\,\mathrm{d}v = \operatorname{erfc} x(\tau|t^*)$. This ansatz is questionable, as the correct potential distribution vanishes beyond the threshold. In view of the widespread use of sigmoidal activation functions in the theory of neural networks (Wilson and Cowan 1972), we nevertheless test a sigmoidal model, but provide it with two free parameters w_1 and w_2:

$$h_{\mathrm{erf}}(\tau|t^*) = w_1\, \mathrm{erfc}[x(\tau|t^*) - w_2] \ , \quad w_1^{\mathrm{opt}} = 0.66\, ,\ w_2^{\mathrm{opt}} = 0.53\ . \tag{13}$$

$\mathrm{erfc}(x) = 1 - \mathrm{erf}(x)$ is the complementary error function. Given the great similarity of the error function and the hyperbolic tangent, we have not extensively investigated the latter. Preliminary results indicate negligible differences (data not shown).

2.2.4 Tuckwell model

Suppose that the input $I(t)$ varies sufficiently slowly so that we may, at any point of time, consider the membrane potential of the neuron to be stationary. A stationary potential $v_0(\tau|t^*)$ corresponds to a constant input current $I_s = v_0(\tau|t^*)$. In this case, the average firing rate, and thus the hazard, can be approximated in closed form (Tuckwell 1989)

$$h_{\mathrm{Tuck}}(\tau|t^*) = \frac{x(\tau|t^*)}{\sqrt{\pi}}\, \mathrm{e}^{-x(\tau|t^*)^2}\, \theta(x(\tau|t^*))\ . \tag{14}$$

The Tuckwell model has no free parameter. The Heaviside step function $\theta(x)$ is introduced to avoid negative values of the hazard. The approximation made in computing the rate is valid only for stimuli far below threshold, i.e. $x(\tau|t^*) \gg 1$. Note that this rate is identical to the diffusive current at the location of the threshold for the threshold free case

$$J_{\mathrm{diff}}(v=1,\tau|t^*) = \frac{\sigma^2}{2}\,\frac{\partial^2}{\partial v^2}\mathcal{P}_f\,(v,\tau\,|\,t^*)\bigg|_{v=1}$$

where $\mathcal{P}_f\,(v,\tau\,|\,t^*)$ is the free Gaussian distribution (7).

2.3 Input

To compare the responses of integrate-and-fire neurons with various hazard functions to those with diffusion noise, we have to choose an input scenario. We will try to be as general as possible and consider time-dependent inputs with both aperiodic and periodic time course. The general form of the input is an oscillatory component of root mean square amplitude q fluctuating around a DC value μ

$$I(t) = \mu + \frac{q\sqrt{2}}{\sqrt{\sum_k \alpha_k^2}} \sum_j \alpha_j \cos(\omega_j t + \phi_j)\ . \tag{15}$$

where $\omega_j = j\,\Delta\omega$ with $\Delta\omega$ the base frequency. Note that $q^2 = \lim_{T\to\infty} \frac{1}{T}\int_0^T (I(t)-\mu)^2 \mathrm{d}t$ is the expected variance of the current. The membrane potential in response to the input in the absence of noise is found from (2)

$$\begin{aligned} v_0(\tau|t^*) &= \mu\left(1-\mathrm{e}^{-\tau}\right) + q\sqrt{2}\left[F(t^*+\tau) - \mathrm{e}^{-\tau}\, F(t^*)\right]\ , \\ F(t) &= \frac{1}{\sqrt{\sum_k \alpha_k^2}} \sum_j \frac{\alpha_j}{\sqrt{1+\omega_j^2}} \sin(\omega_j t + \phi_j + \mathrm{acot}\,\omega_j)\ . \end{aligned} \tag{16}$$

Aperiodic stimuli are characterized by a cut-off frequency Ω_c and are generated by drawing the phases ϕ_j at random from a uniform distribution over $[0, 2\pi)$, while the amplitudes are given by

$$\alpha_j = \begin{cases} 0 & \omega_j \leq 0 \ , \\ 1 & 0 < \omega_j \leq \Omega_c \ , \\ \exp(-\frac{1}{2}(j - j_c)^2) & j_c < j \ . \end{cases} \tag{17}$$

Periodic input is taken to be cosinusoidal with frequency $\Omega = \omega_k$. We set $\alpha_j = \delta_{jk}$ in (15) and obtain

$$I(t) = \mu + q\sqrt{2}\cos(\Omega t + \phi) \ .$$

To compare the performance of the various models across stimuli, we describe each stimulus by its relative distance from threshold

$$\varepsilon = \frac{1 - \left(\mu + \sqrt{2\left\langle \Delta v_0^2 \right\rangle}\right)}{\sigma} \tag{18}$$

where

$$\left\langle \Delta v_0^2 \right\rangle = \lim_{T\to\infty} \int_0^T (v_0(\tau|t^*) - \mu)^2 \mathrm{d}\tau = \frac{q^2}{\sum_k \alpha_k^2} \sum_j \frac{\alpha_j^2}{1 + \omega_j^2}$$

is the rms amplitude of the membrane potential oscillations in the noise-free case. For periodic input, the factor of $\sqrt{2}$ in the definition of ε yields

$$\sigma\varepsilon = 1 - \left(\mu + \frac{q\sqrt{2}}{\sqrt{1+\Omega^2}}\right) = 1 - \sup_{\tau\geq 0} v_0(\tau|t^*) \ .$$

Thus subthreshold stimuli have $\varepsilon > 0$, superthreshold stimuli $\varepsilon < 0$. Note that for periodic stimuli $\varepsilon > 0$ indeed guarantees that the stimulus is subthreshold, i.e. in the absence of noise the neuron never fires. For aperiodic input, however, the definition only holds in a rms sense, so that v_0 may occasionally cross the threshold even for $\varepsilon > 0$.

2.4 Choice of stimuli

The results presented here were obtained from a set of 14,400 periodic and the same number of aperiodic stimuli. DC inputs were in the range $0.55 \leq \mu \leq 1.2$, AC amplitudes approximately $0.1(1-\mu) < q\sqrt{2} < 1.5(1-\mu)$, stimulus/cutoff frequencies $0.02\pi \leq \Omega_c \leq 2\pi$. For each set of these parameters, five phases were chosen randomly from $[0, 2\pi)$ for periodic stimuli, and five different random stimuli generated for aperiodic case. Each stimulus was tested at eight noise amplitudes, randomly chosen so that the stimuli would have a roughly uniform distribution with respect to their relative distance from threshold with $0.1 < |\varepsilon| < 3$. Some two-thirds of all stimuli were subthreshold.

Some stimuli were excluded from analysis. The rejection was based solely on the ISI distributions computed for the diffusion approximation. Specifically, stimuli were excluded if the firing probability was so low, that their norm was insufficient ($\int_0^T \rho(\tau)\mathrm{d}\tau < 0.8$), where T was 20 stimulus periods for periodic and 409.4 for aperiodic stimuli. Furthermore stimuli were rejected if the numerical algorithm was unstable at the time resolution chosen. We verified for some of these case that with appropriate discretization, the algorithm did converge. The instabilities were caused by very steep threshold-crossings of the membrane potential in combination with small noise.

After defective stimuli had been excluded, we were left with 8,714 periodic stimuli (out of these 4,706 subthreshold stimuli) and 12,181 aperiodic stimuli (8,027 subthreshold).

2.5 Parameter optimization

The weights in the models with parameters were chosen as follows. We split the entire set of stimuli into an optimization and a validation set. For each single stimulus, we determined that weight w or set of weights w_1, w_2 that minimized the error E defined in (19) below for this one stimulus, using MATLAB minimization routines. We repeated the procedure for all stimuli in the optimization set and constructed the distribution of weights found in this way. The weights $w^{\rm opt}$ [respectively, $w_1^{\rm opt}, w_2^{\rm opt}$] are the medians of the weight distributions. Evaluating the error E over both the optimization and the validation set with the fixed weight $w^{\rm opt}$ yielded identical results. Overfitting can therefore be excluded.

3 Results

3.1 Inter-spike-interval distributions

Figure 2 shows the ISI distribution evoked from the diffusion model by a sub-threshold aperiodic stimulus. The predicted ISI-distribution for the Arrhenius&Current model (dashed) has been based on (4). To observe this ISI in an experiment, one would present the stimulus shown as dotted line in Fig. 2c repeatedly, starting over at $\tau = 0$ each time a spike has been fired. We may also think of Fig. 2a as a PSTH (Peri-Stimulus-Time Histogram) where each spike triggers a reset of the stimulus.

To measure the agreement between this reference solution and the distributions rendered by the escape noise models, we use the relative integrated mean square error (Scott 1992)

$$E = \frac{\int_0^\infty \mathrm{d}\tau \, [\rho(\tau|t^* = 0) - \rho_{\rm esc}(\tau|t^* = 0)]^2}{\int_0^\infty \mathrm{d}\tau \, \rho(\tau|t^* = 0)^2} \, . \tag{19}$$

Here, $\rho(\tau|t^* = 0)$ is the ISI distribution for the diffusion model, while $\rho_{\rm esc}(\tau|t^* = 0)$ is the distribution obtained from any one of the escape noise models. The example in Fig. 2 corresponds to an error of $E = 0.026$.

Figure 3 shows the cumulative distribution of the error E, for all four models. The Arrhenius&Current model obviously performs significantly better than all the other models for sub- and superthreshold stimuli, both periodic and aperiodic, while the Tuckwell model does worst. The Arrhenius and the error function model are tied for second, with the Arrhenius model yielding slightly smaller errors for superthreshold stimuli. To quantify the performance of the models, we give in table 1 the median and $90^{\rm th}$ percentile of the error for all models. Note that for the Arrhenius&Current model for all stimulus conditions the error is $E < 0.077$ in 90% of all cases. We therefore conclude that this model provides an excellent approximation to the dynamics of the diffusion model of neuronal activity.

We now want to describe in more detail how the model error depends on the stimuli, and briefly discuss why the models perform so differently. Figure 4 shows the error of the models vs. relative distance from threshold of the stimuli, for both periodic and aperiodic stimuli. All models perform better for sub- than for superthreshold stimuli, but the Arrhenius&Current is relatively good across the entire range. Note that the Tuckwell model becomes quite good for periodic stimuli which are far below threshold ($\varepsilon > 1$), as is to be expected, since the Tuckwell approximation is valid in this regime. It does not fare

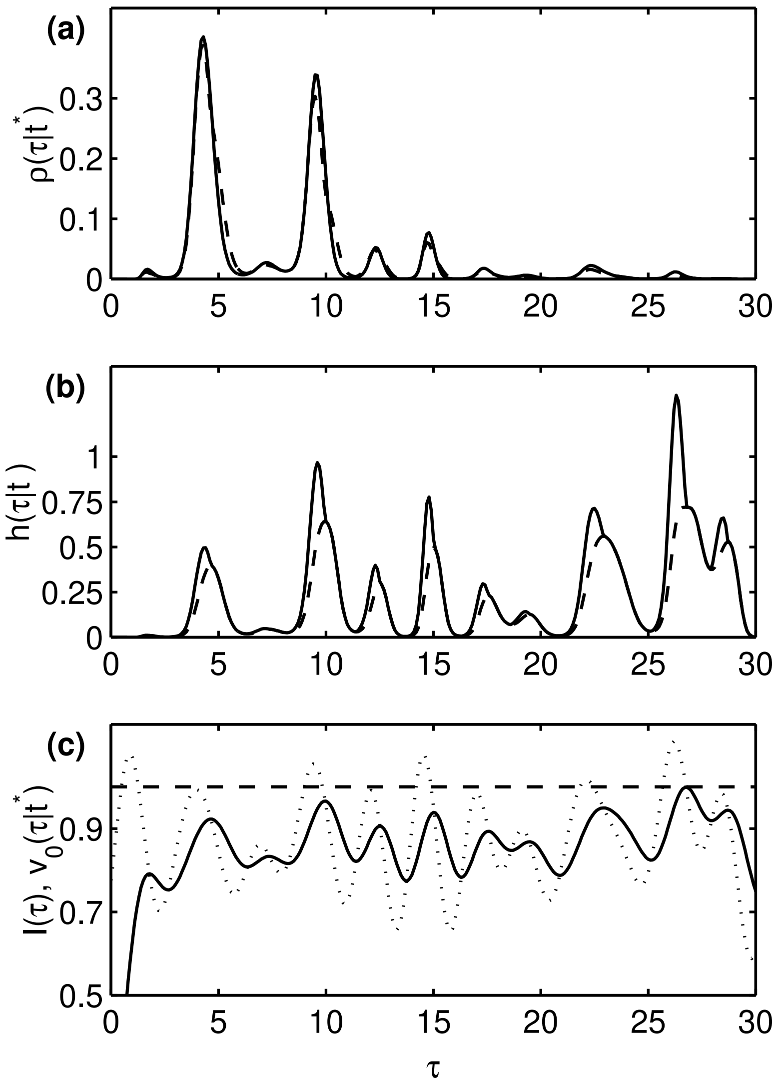

Figure 2: (a) Interval distribution from the diffusion model (solid) and the Arrhenius&Current model (dashed) for aperiodic input with DC offset $\mu = 0.85$, AC amplitude $q = 0.1$, cutoff frequency $\Omega_c = \pi$ and noise amplitude $\sigma = 0.1$. The relative distance from threshold is $\varepsilon = 0.88$ and the error $E = 0.026$. (b) Hazard as a function of time for the Arrhenius&Current model (solid). The dashed line is the diffusive component of the hazard defined in Eq. (12). (c) Input current (dotted) and noise-free membrane potential for the given stimulus (solid). The membrane potential stays below the threshold (dashed), but approaches it closely around $\tau \approx 27$. Note that peaks in the input current in (c) lead to sharp transients of the hazard (b) that would not be reproduced correctly by the diffusion term alone. Thus the firing probability of the neuron is correlated to maxima of the current rather than the membrane potential, in excellent agreement with the exact diffusion model; see the nice fit in (a).

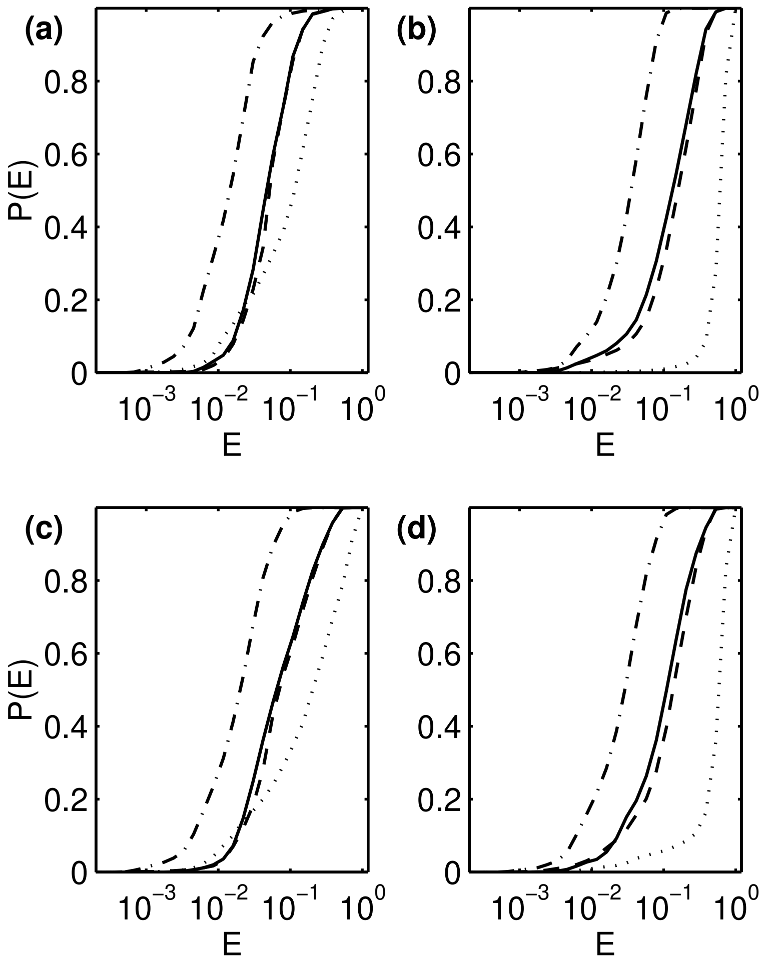

Figure 3: Cumulative distribution of the relative mean square error E over all stimuli for Arrhenius (solid), Arrhenius&Current (dash-dotted), error function (dashed) and Tuckwell (dotted) model. The stimuli were (a) subthreshold periodic, (b) superthreshold periodic, (c) subthreshold aperiodic and (d) superthreshold aperiodic. To interpret the cumulative distributions, let us study the likelihood that the error E of our approximation is smaller than 0.1. We may read off from the graphs in, e.g. (a), that for subthreshold periodic stimuli, the Tuckwell model would give a probability of $E \leq 0.1$ of about 50 percent, whereas the Arrhenius model and the error function give about 80 percent and the Arrhenius&Current model a probability of more than 95 percent.

	per, sub		aper, sub		per, super		aper, super		overall	
	50%	90%	50%	90%	50%	90%	50%	90%	50%	90%
Arr	0.055	0.148	0.075	0.336	0.157	0.409	0.130	0.375	0.091	0.334
A&C	0.018	0.044	0.024	0.070	0.042	0.090	0.034	0.090	0.026	0.077
erf	0.061	0.147	0.083	0.346	0.189	0.429	0.160	0.397	0.103	0.358
Tuck	0.137	0.333	0.242	0.837	0.747	0.896	0.713	0.901	0.398	0.864

Table 1: Median (= 50^{th}) and 90^{th} percentiles of errors E for the different stimulus conditions and for all conditions combined. E.g., for the Arrhenius&Current model with periodic superthreshold input, $E < 0.042$ in 50% of all cases, and $E > 0.090$ for only 10% of the stimuli tested.

as well for aperiodic stimuli, for they may contain intervals during which the membrane potential of a subthreshold stimulus comes close to threshold.

3.2 Stochastic resonance

Recent years have seen mounting evidence that signal transmission in neurons can be improved by noise, an effect known as stochastic resonance (Douglass et al. 1993; Wiesenfeld and Moss 1995; Cordo et al. 1996; Levin and Miller 1996; Moss and Russell 1998). The typical experimental paradigm is to stimulate a neuron sinusoidally, adding noise of varying intensity, and to measure the signal-to-noise ratio (SNR) of the spike train elicited from the neuron. If this SNR peaks for non-vanishing input noise, the system is said to exhibit stochastic resonance. For a recent review of the field, see Gammaitoni et al. (1998).

Plesser and Geisel (1998) have demonstrated that noise can induce a further kind of resonance in periodically stimulated integrate-and-fire neurons: the optimal SNR is attained for a particular stimulation frequency. This latter resonance arises by matching the period of stimulation to the time-scale set by the membrane time constant of the neuron. We shall show here that the simplified Arrhenius&Current model reproduces this behavior well, and that it is thus well suited to investigate integrate-and-fire dynamics. For details of the methods, we refer the reader to Plesser and Geisel (1998).

Briefly, one proceeds as follows to obtain the SNR in response to sinusoidal stimulation: For periodic input $I(t) = \mu + q\cos(\Omega t + \phi)$ the inter-spike-interval distributions $\rho(\tau|t^*, I(\cdot))$ depend on input and external time only through the input phase $\psi^* = [\Omega t^* + \phi_0] \bmod 2\pi$ at the time t^* of the most recent spike. With respect to this *spike phase*, the spike train reduces to a Markov process with transition probability (or kernel)

$$\mathcal{T}(\psi_k|\psi_{k-1}) = \int_0^\infty \rho(\tau|\psi_{k-1})\delta(\psi_k - [\Omega\tau + \psi_{k-1}] \bmod 2\pi)\frac{\mathrm{d}\tau}{\Omega} \tag{20}$$

between the phases of the k^{th} and the $k-1^{\text{st}}$ spike. The power spectral density at the stimulus frequency Ω of a δ-spike train of total length T_o is then given by

$$S_{T_o}(\Omega) = \frac{1}{\pi T_o}\left\langle \sum_{j,k}^{t_j,t_k<T_o} \mathrm{e}^{i\Omega(t_j-t_k)} \right\rangle \approx \frac{1}{\pi N_o \langle\tau\rangle}\left\langle \sum_{j,k=1}^{N_o} \mathrm{e}^{i(\psi_j-\psi_k)} \right\rangle \ . \tag{21}$$

Here, t_j are the spike times, ψ_j the spike phases and we have exploited that $\psi_j - \psi_k = [\Omega(t_j - t_k)] \bmod 2\pi$. The mean inter-spike interval length is given by $\langle\tau\rangle$ and $N_o = \lfloor T_o/\langle\tau\rangle \rfloor$

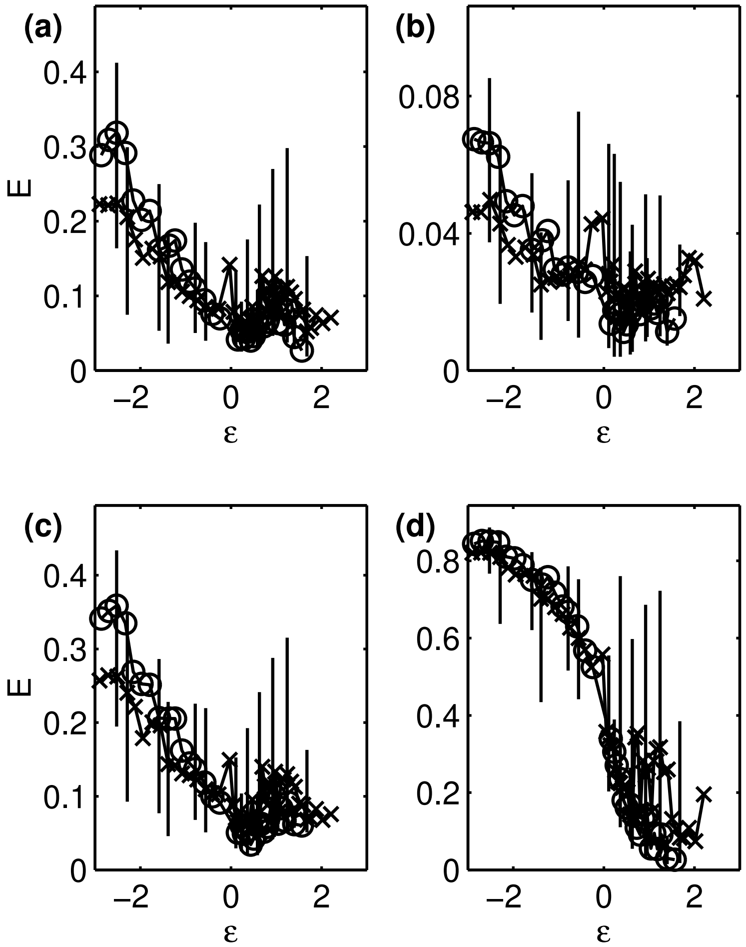

Figure 4: Error E vs. relative distance from threshold ε for (a) Arrhenius, (b) Arrhenius&Current, (c) error function and (d) Tuckwell model. Symbols mark the medians, and vertical bars span the 20^{th} to 80^{th} percentiles of 250 stimuli with neighboring ε-values. Circles indicate periodic stimuli, crosses aperiodic ones. $\varepsilon > 0$ corresponds to the regime of subthreshold stimuli. Note the different scales of the y-axis.

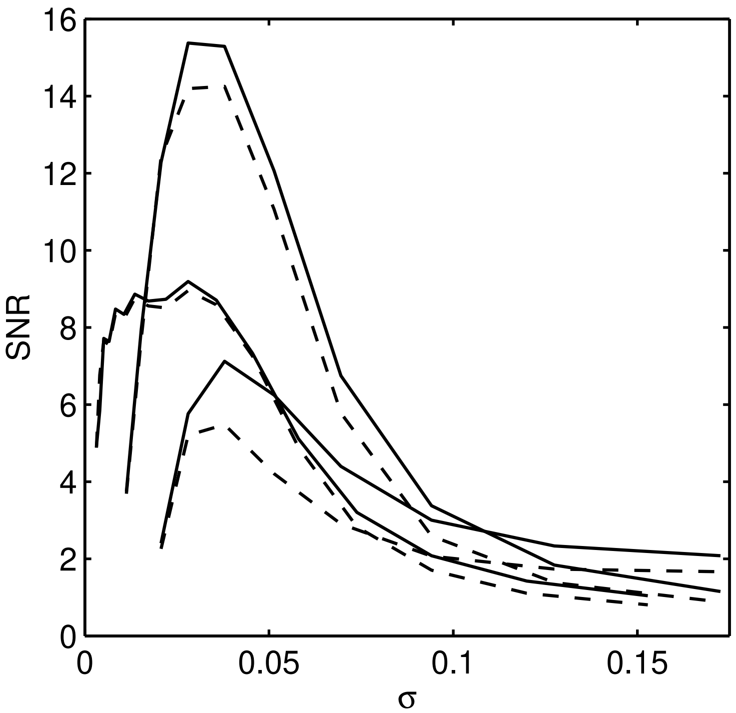

Figure 5: Signal-to-noise ratio SNR vs. noise amplitude σ for $\mu = 0.95$, $q\sqrt{2} = 0.05$ and $\Omega = 0.33\pi$ (highest SNR), $\Omega = \pi$ (lowest SNR) and $\Omega = 0.1\pi$. Solid lines are for the diffusion model, dashed lines for the Arrhenius&Current model.

is the average number of spikes in T_o. The approximation in equation (21) consists in averaging the number of spikes in T_o and their phases separately. Since the correlations between the spike phases ψ_j are given by (20), the right-hand side of equation (21) can be evaluated in closed form. Results are in excellent agreement with spectra computed via FFT from simulated spike trains.

As an estimate of the noise background on which this signal will be transmitted, we use the power spectral density of a Poisson process of the same mean number of spikes per time as the spike train studied in equation (21); see Stemmler (1996). A Poisson process with intensity $\langle\tau\rangle^{-1}$ has a white spectrum with power $S_P = (\pi\langle\tau\rangle)^{-1}$, see Cox and Lewis (1966). The signal-to-noise ratio of a spike train transmitted within a fixed observation period T_o is then

$$\mathrm{SNR} = \frac{S_{T_o}(\Omega)}{S_P} \approx \frac{1}{N_o}\left\langle \sum_{j,k=1}^{N_o} \mathrm{e}^{i(\psi_j - \psi_k)} \right\rangle .$$

Figure 5 shows results for the integrate-and-fire model with diffusion noise and Arrhenius&Current escape noise. The agreement is good, indicating that the Arrhenius&Current model is well suited to replace diffusive noise in the integrate-and-fire neuron when investigating more intricate problems of neuronal dynamics. Note in particular that both models show a two-fold stochastic resonance. The SNR exhibits, as always in stochastic resonance, a peak as a function of the noise amplitude. The height of this peak is maximal around a stimulus frequency $\Omega = 0.33\pi$ and decreases both for larger ($\Omega = \pi$) and smaller frequencies ($\Omega = 0.1\pi$). The optimal frequency $\Omega = 0.33\pi$ corresponds to a period of $T = 6$, which should be compared to the mean inter-spike-interval length $\langle\tau\rangle \approx 9.7$ at the resonance. For a more detailed discussion of the timescale matching underlying this effect, see Plesser and Geisel (1998).

4 Discussion

We have demonstrated above that the dynamics of the integrate-and-fire neuron with diffusive noise may be well approximated by simple escape noise models, and have identified the Arrhenius&Current hazard function as the optimal choice of model. Upon periodic stimulation, the signal-to-noise ratio of the neuron's output exhibits stochastic resonance for the Arrhenius&Current noise in the same way as it does for diffusive noise. This indicates that this escape noise model renders the correlations within the spike train—induced by the time-dependent stimulus—correctly. The relative error of the model depends only weakly on the stimulus, permitting for a widespread use.

Of the remaining models, the pure Arrhenius model finishes as a strong second, at least for subthreshold stimuli. Compared to the error function model, it has the additional charm of mathematical simplicity. The model based on Tuckwell's approximation of the mean firing rate, in contrast, is useful only if stimuli are sufficiently subthreshold.

With this study, we have provided a tool for the efficient investigation of large networks of model neurons. As a matter of fact, escape noise models have been used in the past in the context of the Spike Response Model (Gerstner and van Hemmen 1992; Gerstner 1995), and this study provides additional support to such simplified treatment of noise. For escape noise models, signal transmission properties of spiking neurons can be studied analytically (Gerstner 1998a). Several issues remain to be tackled, particularly the extension of the present investigation to the case of colored noise. Finally, while the Arrhenius&Current model is the best model we have found so far, this is as yet no proof that it is indeed the optimal model.

Acknowledgements

We acknowledge helpful comments by two anonymous referees on an earlier version of the manuscript. HEP was supported by Deutsche Forschungsgemeinschaft through SFB 185 "Nichtlineare Dynamik".

References

Abeles, M. (1982). Role of the cortical neuron: integrator or coincidence detector. *Israel J Med Sci 18*, 83–92.

Brunel, N. and V. Hakim (1998). Fast global oscillations in networks of integrate-and-fire neurons with low firing rates. To appear in *Neural Computation*.

Bryant, H. L. and J. P. Segundo (1976). Spike inititation by transmembrane current: a white-noise analysis. *J Physiol 260*, 279–314.

Bulsara, A. R. and A. Zador (1996). Threshold detection of wideband signals: A noise-induced maximum in the mutual information. *Phys Rev E 54*, R2185–R2188.

Collins, J. J., C. C. Chow, A. C. Capela, and T. T. Imhoff (1996). Aperiodic stochastic resonance. *Phys Rev E 54*, 5575–5584.

Cordo, P., J. T. Inglis, S. Verschueren, J. J. Collins, D. M. Merfeld, S. Rosenblum, S. Buckley, and F. Moss (1996). Noise in human muscle spindels. *Nature 383*, 769–770.

Cox, D. R. and P. A. W. Lewis (1966). *The Statistical Analysis of Series of Events*. London: Methuen.

Douglass, J. K., L. Wilkens, E. Pantazelou, and F. Moss (1993). Noise enhancement of information transfer in crayfish mechanoreceptors by stochastic resonance. *Nature 365*, 337–340.

Gammaitoni, L., P. Hänggi, P. Jung, and F. Marchesoni (1998). Stochastic resonance. *Rev Mod Phys 70*, 223–287.

Gerstner, W. (1995). Time structure of the activity in neural network models. *Phys Rev E 51*, 738–758.

Gerstner, W. (1998a). Population dynamics of spiking neurons: fast transients, asynchronous states, and locking. To appear in *Neural Computation*.

Gerstner, W. (1998b). Spiking neurons. In W. Maass and C. M. Bishop (Eds.), *Pulsed Neural Networks*, Chapter 1, pp. 3–54. Cambridge, MA: MIT Press.

Gerstner, W. and J. L. van Hemmen (1992). Associative memory in a network of 'spiking' neurons. *Network 3*, 139–164.

Gummer, A. W. (1991). Probability density function of successive intervals of a nonhomogeneous Poisson process under low-frequency conditions. *Biol Cybern 65*, 23–30.

Johannesma, P. I. M. (1968). Diffusion models of the stochastic activity of neurons. In E. R. Caianiello (Ed.), *Neural Networks*, pp. 116–144. Berlin: Springer.

Johnson, D. H. (1980). The relationship between spike rate and synchrony in responses of auditory-nerve fibers to single tones. *J Acoust Soc Am 68*, 1115–1122.

Johnson, D. H. (1996). Point process models of single-neuron discharges. *J Comp Neurosci 3*, 275–299.

Kempter, R., W. Gerstner, J. L. van Hemmen, and H. Wagner (1998). Extracting out oscillations: neural coincidence detection with periodic spike input. *Neural Comp 10*, 1987–2017.

König, P., A. K. Engel, and W. Singer (1996). Integrator or coincidence detector? The role of the cortical neuron revisited. *Trends Neurosci 19*(4), 130–137.

Lánský, P. (1997). Sources of periodical force in noisy integrate-and-fire models of neuronal dynamics. *Phys Rev E 55*, 2040–2043.

Levin, J. E. and J. P. Miller (1996). Broadband neural encoding in the cricket cercal sensory system enhanced by stochastic resonance. *Nature 380*, 165–168.

Linz, P. (1985). *Analytical and Numerical Methods for Volterra Equations.* Philadelphia: SIAM.

Mainen, Z. F. and T. J. Sejnowski (1995). Reliability of spike timing in neocortical neurons. *Science 268*, 1503–1506.

Moss, F. and D. F. Russell (1998). Animal behavior enhanced by noise. Computational Neuroscience Meeting '98, Santa Barbara, CA, July 1998.

Perkel, D. H., G. L. Gerstein, and G. P. Moore (1967). Neuronal spike trains and stochastic point processes. *Biophys J 7*, 391–418.

Plesser, H. E. and T. Geisel (1998). Markov analysis of stochastic resonance in a periodically driven integrate-fire neuron. To appear in *Phys Rev E*, preprint at http://xxx.lanl.gov, physics/9810019.

Plesser, H. E. and S. Tanaka (1997). Stochastic resonance in a model neuron with reset. *Phys Lett A 225*, 228–234.

Rieke, F., D. Warland, R. de Ruyter van Steveninck, and W. Bialek (1997). *Spikes: Exploring the Neural Code.* Cambridge, MA: MIT Press.

Scott, D. W. (1992). *Multivariate Density Estimation.* New York: Wiley.

Siebert, W. M. (1970). Frequency discrimination in the auditory system: Place or periodicity mechanisms. *Proc IEEE 58*, 723–730.

Stein, R. B. (1965). A theoretical analysis of neuronal variability. *Biophys J 5*, 173–194.

Stemmler, M. (1996). A single spike suffices: the simplest form of stochastic resonance in neuron models. *Network 7*, 687–716.

Stevens, C. F. and A. Zador (1996). When is an integrate-and-fire neuron like a Poisson neuron? In D. S. Touretzky, M. C. Mozer, and M. E. Hasselmo (Eds.), *Advances in Neural Information Processing Systems*, Volume 8, pp. 103–109. The MIT Press.

Tuckwell, H. C. (1988). *Introduction to Theoretical Neurobiology*, Volume 1. Cambridge, UK: Cambridge University Press.

Tuckwell, H. C. (1989). *Stochastic Processes in the Neurosciences.* Philadelphia: SIAM.

van Kampen, N. G. (1992). *Stochastic Processes in Physics and Chemistry* (second ed.). Amsterdam: North-Holland.

van Vreeswijk, C. and H. Sompolinski (1996). Chaos in neuronal networks with balanced excitatory and inhibitory activity. *Science 274*, 1724–1726.

Wiesenfeld, K. and F. Moss (1995). Stochastic resonance and the benefits of noise: from ice ages to crayfish and SQUIDs. *Nature 373*, 33–36.

Wilson, H. R. and J. D. Cowan (1972). Excitatory and inhibitory interactions in localized populations of model neurons. *Biophys J 12*, 1–24.